

## Thermodynamic properties of fluid sodium from molecular dynamics

Galen K. Straub, Sheila K. Schiferl, and Duane C. Wallace  
*Los Alamos National Laboratory, Los Alamos, New Mexico 87545*  
 (Received 22 March 1983)

The high-temperature thermodynamic properties of metallic fluid sodium were calculated from melting to a temperature  $T=2200$  K. A pseudopotential model was used that consisted of a large volume-dependent potential plus a small effective two-body potential. Using molecular-dynamics calculations for the ionic motions and including electronic excitation contributions, we have determined the zero-pressure volume versus temperature curve, the adiabatic bulk modulus, the heat capacities at constant pressure and volume, and the thermodynamic Grüneisen parameter. We find our theory to be in excellent agreement with experiment up to  $T=1200$  K, but note a significant deviation at higher temperatures.

### I. INTRODUCTION

In our previous work, the thermodynamic properties of solid metallic sodium<sup>1</sup> and the pressure-temperature melting-phase line<sup>2</sup> were studied using a pseudopotential model of metallic sodium. The high-temperature ionic vibrational motion was calculated using molecular dynamics. In the present paper we extend our previous study to include the high-temperature fluid phase of sodium. With the use of the same potential for the fluid phase as was previously used for the solid phase, a comprehensive series of molecular-dynamics calculations was done above the melting temperature  $T_M$ .

Several previous studies on the thermodynamics of liquid metals have been done.<sup>3</sup> Jones<sup>4</sup> has used hard-sphere perturbation theory to calculate several thermodynamic properties of sodium near  $T_M$ , and the heat capacity and sound speed to about  $T=1500$  K. Mountain<sup>5</sup> has done Monte Carlo simulations to  $T=500$  K, but only at a single volume. In our work we have used molecular dynamics to calculate the thermodynamic properties of fluid sodium from  $T_M$  to  $T=2200$  K. Our theory is in excellent agreement with experiment to about  $T=1200$  K, above which we note a significant departure of theory and experiment. In Sec. II we discuss the method for determining the total pressure and energy using molecular dynamics, as well as the calculation of the heat capacities, Grüneisen parameter, and isothermal bulk modulus. Section III contains the comparisons with experiment of our theory along the zero-pressure line.

### II. METHOD

Our system consists of  $N$  ions and  $NZ$  electrons in a volume  $V$ . We use the adiabatic approximation to express the total energy as the sum of the ionic kinetic energy plus the total adiabatic potential  $\Phi$ . The adiabatic potential is evaluated in the pseudopotential perturbation formulation, which yields a volume-dependent term  $\Omega(V)$  and a sum over all distinct pairs of ions of the effective ion-ion potential  $\phi(r;V)$ . The total adiabatic potential becomes

$$\Phi - NI_Z = \Omega(V) + \sum \phi(r;V), \quad (1)$$

where we have taken the zero of  $\Phi$  to correspond to a system of neutral atoms at infinite separation, and  $I_Z$  is the ionization energy. Expressions for  $\Omega(V)$  and  $\phi(r;V)$  are given by Eqs. (2) and (3) of Ref. 1.

We have used the same potential for our study of sodium's fluid-phase thermodynamics as was used for the solid bcc phase.<sup>6</sup> A graph of  $\phi(r;V)$  for Na is shown in Fig. 1 for several different values of the atomic  $V_a$ . The zero-temperature-pressure volume is  $256a_0^3$ , and the curves cover the volume range of our study. The total internal energy is

$$U = \langle E_{\text{ion}}^{\text{kin}} \rangle + \langle \Phi \rangle + U_e, \quad (2)$$

where  $E_{\text{ion}}^{\text{kin}}$  is the kinetic energy of the ions and the total pressure is

$$P = -\frac{d\Omega}{dV} + \frac{NkT}{V} - \left\langle \sum \left[ \frac{\partial \phi}{\partial V} + \frac{r}{3V} \frac{\partial \phi}{\partial r} \right] \right\rangle + P_e. \quad (3)$$

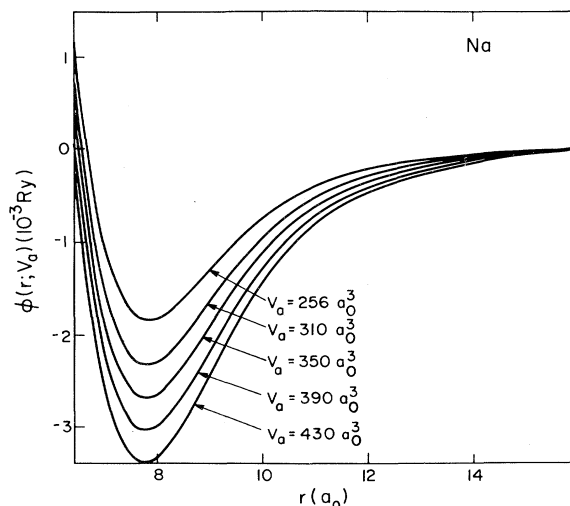


FIG. 1. Total effective pair potential for Na calculated from the modified point-ion pseudopotential. The zero-temperature volume is  $V_a=256a_0^3$ . The potential energy is in units of rydbergs (Ry) and the separation is in units of Bohr radii ( $a_0$ ).

The summation is again over all distinct pairs of ions and the angular brackets denote an ensemble average.  $k$  is Boltzmann's constant.  $U_e$  and  $P_e$  are the electron-gas contributions to the internal energy and pressure, respectively.<sup>7</sup>

The electronic terms result from the thermal excitation of the conduction-electron gas and become important in the high-temperature fluid region. The electronic internal energy is given by

$$U_e = \frac{1}{2} \Gamma T^2, \quad (4)$$

and the pressure is given by

$$P_e V = \frac{2}{3} U_e = \frac{1}{3} \Gamma T^2. \quad (5)$$

$\Gamma$  was evaluated in the free-electron approximation from the expression

$$\Gamma = \frac{N \pi^2 k^2 m Z}{\hbar^2 f^2}, \quad (6)$$

where  $m$  is the electron mass and  $f$  is the free-electron Fermi wave number. Because of the fairly strong temperature dependence of the electronic terms, they cannot be neglected in the fluid phase; their inclusion improves the agreement between theory and experiment.  $P_e$  becomes nearly 3% of the ionic contribution to the pressure at  $T = 1800$  K.

Equations (2) and (3) are evaluated from molecular-dynamics simulations on a calculational cell consisting of 686 particles in a cubic volume with periodic boundary conditions in all directions. The coupled classical equations of motion are solved numerically in the central finite-difference approximation under the constraints of constant total energy and volume. When the system is in equilibrium, the temperature  $T$  is related to the molecular-dynamics ensemble-average (indicated by angular brackets with subscripts MD) kinetic energy by

$$\frac{3}{2} k T = N^{-1} \langle E_{\text{ion}}^{\text{kin}} \rangle_{\text{MD}} + O(N^{-1}). \quad (7)$$

Here  $T$  is the temperature in the generalized canonical ensemble and  $O(N^{-1})$  gives the size-dependent corrections for evaluating the temperature from the molecular-dynamics ensemble.<sup>8</sup> Note that  $\langle E_{\text{ion}}^{\text{kin}} \rangle_{\text{MD}}$  is of  $O(N)$  and hence the average kinetic energy per particle  $N^{-1} \langle E_{\text{ion}}^{\text{kin}} \rangle_{\text{MD}}$  is of relative order  $O(1)$ .

Molecular-dynamics calculations were done at six different volumes in the fluid phase and over a temperature range from melting,  $T_M$ , to  $T = 2200$  K. The results for the internal energy and pressure are given in Figs. 2 and 3, respectively. Both plots include the electronic contributions given by Eqs. (4)–(6). Table I lists  $\Omega(V)$  and its volume derivative at the six volumes.

At each volume,  $U$  and  $P$  were fitted to cubic polynomials as a function of temperature. From these fits, the heat capacity at constant volume

$$C_V = \left[ \frac{\partial U}{\partial T} \right]_V, \quad (8)$$

and the thermodynamic Grüneisen parameter

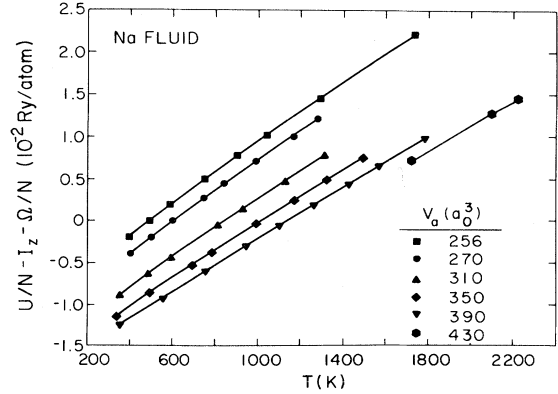


FIG. 2. Total internal energy per atom  $U/N$  minus the ionization energy  $I_Z$  and the volume-dependent portion of the potential  $\Omega(V)/N$  vs temperature from the molecular-dynamics calculations. Values of  $\Omega(V)/N$  are given in Table I. Each plotting symbol represents a single molecular-dynamics calculation. The electronic contributions given by Eq. (4) have been included.

$$\gamma = V \left[ \frac{\partial P}{\partial U} \right]_V = V \frac{(\partial P / \partial T)_V}{(\partial U / \partial T)_V}, \quad (9)$$

may be evaluated directly.

The collection of polynomial fits at constant volumes was also used to generate sets of points at constant temperatures. These new sets of points were similarly fitted to polynomials as functions of volume, giving  $U$  and  $P$  as functions of volume at constant temperatures. Both the fits at constant volume and constant temperature were done to high numerical accuracy, allowing a complete description of the fluid phase as a continuous function of  $T$  and  $V$ . The isothermal bulk modulus

$$B_T = -V \left[ \frac{\partial P}{\partial V} \right]_T, \quad (10)$$

and the heat capacity at constant pressure

$$C_P = C_V + \frac{T \gamma^2 C_V^2}{V B_T}, \quad (11)$$

can then be evaluated from our fitted functions.

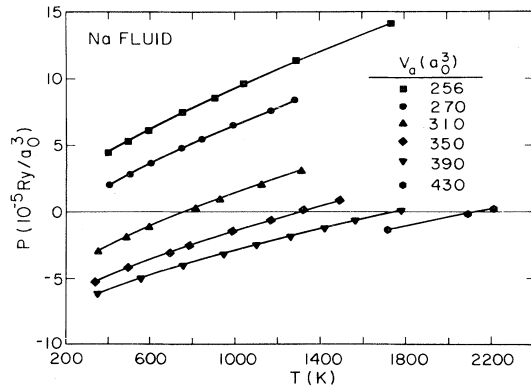


FIG. 3. Total pressure  $P$  vs temperature from the molecular-dynamics calculations. The electronic contributions from Eq. (5) have been included.

TABLE I. Volume-dependent contribution  $\Omega(V)$  to the total energy and its first derivative.

$V_a$ ( $a_0^3/\text{atom}$ )	$\Omega(V_a)/N$ (Ry/atom)	$d\Omega/dV$ ( $10^{-4}$ Ry/ $a_0^3$ )
256	-0.463 209	1.547 54
270	-0.461 087	1.486 18
310	-0.455 452	1.336 68
350	-0.450 354	1.216 50
390	-0.445 692	1.117 63
430	-0.441 392	1.034 72

In the present work we have not determined the Helmholtz free energy itself, but instead have calculated the thermodynamic functions directly from derivatives of the total energy and pressure. The procedure for calculating the Helmholtz function and the entropy constant, from the high-temperature cluster expansion of the pressure and energy, is given in Ref. 9.

### III. COMPARISON WITH EXPERIMENT

Using the fitting procedure described in the preceding section for representing the molecular-dynamics results plus electronic contributions, we have determined the zero-pressure volume as a function of temperature. Our result is given in Fig. 4 along with the experimental data of Gol'tsova<sup>10</sup> and of Dillon, Nelson, and Swanson.<sup>11</sup> The theoretical curve is in excellent agreement with experiment from  $T_M$  to  $T=1200$  K. Above  $T=1200$  K, our theoretical results definitely depart from experiment. The maximum discrepancy of 15% occurs at the highest temperature of  $T=2200$  K.

The thermodynamic properties of the fluid phase of sodium were calculated along the  $P=0$  line and compared with experiment. Figure 5 is a plot of the isothermal bulk modulus  $B_T$ , and Fig. 6 shows the heat capacities  $C_V$  and  $C_P$ . The experimental data for  $B_T$  are given in Refs. 12-16, and the heat-capacity data were taken from Ginnings, Douglas, and Ball.<sup>17</sup> The agreement with experiment is very good; at  $T=1100$  K, our theoretical values of

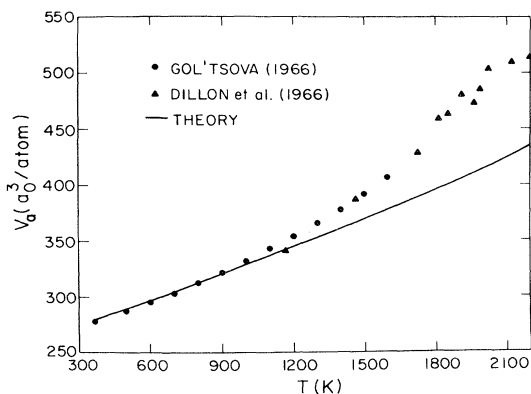


FIG. 4. Calculated and measured values of the volume vs temperature at  $P=0$ .

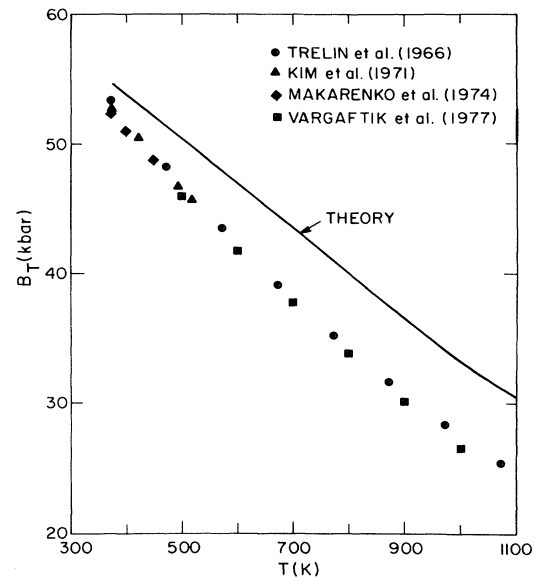


FIG. 5. Isothermal bulk modulus  $B_T$  vs temperature along the  $P=0$  curve.

$B_T$  and  $C_P$  have a maximum deviation from experiment of 15% and 9%, respectively.

The thermodynamic Grüneisen parameter  $\gamma$  was also calculated along the zero-pressure curve and is compared with experiment in Fig. 7. The experimental points were determined from experimental values of the thermal expansion, isothermal bulk modulus, and heat capacity at constant volume, using the procedure described previously.<sup>1</sup> Our molecular-dynamic results are again in good quantitative agreement with experiment and have a 7% deviation at the highest experimental point. A frequent assumption used in constructing an equation of state from shock-wave data is that  $\gamma$  times the density  $\rho$  is a constant.

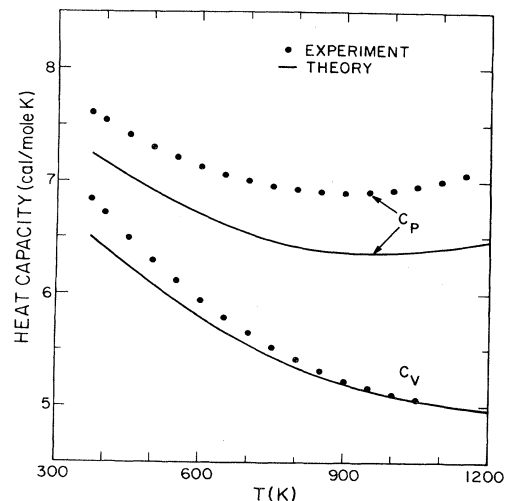


FIG. 6. Heat capacity at constant pressure  $C_P$  and the heat capacity at constant volume  $C_V$  vs temperature. The experimental points were determined from Ref. 17.

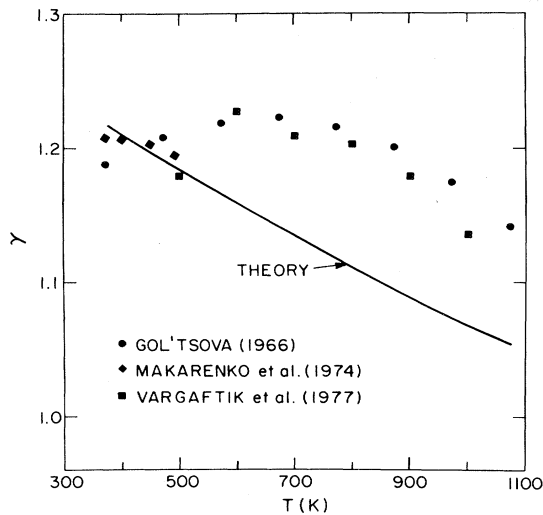


FIG. 7. Thermodynamic Grüneisen parameter  $\gamma$  vs temperature. The experimental points (Refs. 10 and 14–16) shown are determined from experimental values of the thermal expansion, isothermal bulk modulus, and heat capacity at constant volume.

Our theoretical results show that  $\rho\gamma$  decreases by about 30% between  $T_M$  and  $T=1200$  K.

#### IV. CONCLUSIONS

From our comparison of theory and experiment over an extended range of both temperature and volume, we can make the following conclusions.

(1) An adiabatic potential energy evaluated from pseudopotential theory, along with molecular-dynamics simulations for the ionic motion, provides an accurate description of fluid metallic sodium over the range of volume  $V_a = 256a_0^3$ – $350a_0^3$ , and from  $T_M$  to  $T=1200$  K.

(2) The potential used in the fluid calculations is the same as was previously used to determine accurately the high-temperature anharmonic properties of crystalline Na to  $T_M^1$ , the solid-fluid phase boundary,<sup>2</sup> and the low-temperature thermodynamic properties.<sup>6</sup> Thus, we conclude that we have an excellent theoretical understanding

of the thermodynamic behavior of metallic sodium between  $T=0$  and  $T=1200$  K.

(3) Above  $T=1200$  K, our theory significantly deviates from experiment. One possibility is the failure of the pseudopotential method when the volume becomes too large. To investigate this possibility, we have studied the linear muffin-tin orbital (LMTO) electronic band calculations for sodium done by Albers.<sup>18</sup> Albers's LMTO calculations cover the volume range where our theoretical  $V_a$ -vs- $T$  curve (Fig. 4) deviates from experiment and we can compare the LMTO results with the predictions of pseudopotential theory.

The pseudopotential method will fail when the system of electrons is no longer describable by a nearly free-electron theory. As the volume continues to increase, ultimately we will have isolated atoms with a single 3s electron on each atom and an insulating system. For the entire range of volumes studied, we find no evidence of electron localization and have the following indications for normal metallic behavior. First, the Fermi energy as a function of volume from LMTO calculations is in excellent agreement with our pseudopotential model using perturbation theory.<sup>19</sup> Second, the bandwidth of the 3s band at  $V_a = 570a_0^3$  is 0.4 Ry. Third, the spherical radius for the average volume per electron,  $r_s$ , is in the metallic range with  $r_s = 5a_0$  at the largest volume. Fourth, the discrepancy between theory and experiment at  $V_a = 430a_0^3$  in Fig. 4 represents only a 2.1-kbar difference in the total pressure. Thus we conclude that the pseudopotential method is valid for the volumes investigated.

The most likely explanation for the deviation of our calculation from experiment above  $T=1200$  K is due to the extensive extrapolation of our pseudopotential model to large volumes. The model parameters were fitted to experimental data at  $V_a = 256a_0^3$  (normal density). With a relatively small adjustment of the model parameters, one could account for the 2.1-kbar discrepancy at  $V_a = 430a_0^3$ .

#### ACKNOWLEDGMENTS

We would like to thank R. Albers, B. Holian, and J. D. Johnson for valuable comments and discussions. This work was supported by the U.S. Department of Energy.

<sup>1</sup>R. E. Swanson, G. K. Straub, B. L. Holian, and D. C. Wallace, *Phys. Rev. B* **25**, 7807 (1982).

<sup>2</sup>B. L. Holian, G. K. Straub, R. E. Swanson, and D. C. Wallace, *Phys. Rev. B* **27**, 2873 (1983).

<sup>3</sup>For a review of liquid-metal theory, see N. W. Ashcroft and D. Stroud, in *Solid State Physics*, edited by H. Ehrenreich, F. Seitz, and D. Turnbull, (Academic, New York, 1978), Vol. 33, p. 1.

<sup>4</sup>H. D. Jones, *Phys. Rev. A* **8**, 3215 (1973).

<sup>5</sup>R. D. Mountain, *Seventh Symposium on Thermophysical Properties*, edited by A. Cezairliyan (American Society of Mechanical Engineers, New York, 1977), p. 878.

<sup>6</sup>D. C. Wallace, *Phys. Rev.* **176**, 832 (1968).

<sup>7</sup>D. C. Wallace, *Thermodynamics of Crystals*, (Wiley, New York, 1972).

<sup>8</sup>D. C. Wallace and G. K. Straub, *Phys. Rev. A* **27**, 2201 (1983).

<sup>9</sup>D. C. Wallace, B. L. Holian, J. D. Johnson, and G. K. Straub, *Phys. Rev. A* **26**, 2882 (1982).

<sup>10</sup>E. I. Gol'tsova, *Teplofiz. Vys. Temp.* **4**, 360 (1966) [*High Temp. (USSR)* **4**, 348 (1966)].

<sup>11</sup>I. G. Dillon, P. A. Nelson, and B. S. Swanson, *J. Chem. Phys.* **44**, 4229 (1966).

<sup>12</sup>Y. S. Trelin, I. N. Vasil'ev, V. B. Proskurin, and T. A. Tsyganova, *Teplofiz. Vys. Temp.* **4**, 364 (1966) [*High Temp. (USSR)* **4**, 352 (1966)].

<sup>13</sup>M. G. Kim, K. A. Kemp, and S. V. Letcher, *J. Acoust. Soc. Am.* **49**, 706 (1971).

<sup>14</sup>I. N. Makarenko, A. M. Nikolaenko, and S. M. Stishov, *Phys. Lett.* **49A**, 257 (1974).

<sup>15</sup>I. N. Makarenko, A. M. Nikolaenko, V. A. Ivanov, and S. M. Stishov, *Zh. Eksp. Teor. Fiz.* **69**, 1723 (1975) [*Sov. Phys.—JETP* **42**, 875 (1975)].

<sup>16</sup>N. B. Vargaftik, V. F. Kozhevnikov, V. G. Stepanov, V. A. Alekseev, and Y. F. Ryzhkov, *Seventh Symposium on Thermophysical Properties*, edited by A. Cezairliyan (American Society of Mechanical Engineers, New York, 1977).

<sup>17</sup>D. C. Ginnings, T. B. Douglas, and A. F. Ball, *J. Res. Natl. Bur. Stand.* **45**, 23 (1950).

<sup>18</sup>R. Albers (private communication).

<sup>19</sup>Equation (26.56) of Ref. 7.